Fluorescence Modulation of Single CdSe Nanowires by Charge Injection through the Tip of an Atomic-Force Microscope

Sebastian Schäfer, Zhe Wang, Tobias Kipp, and Alf Mews

Institute of Physical Chemistry, University of Hamburg, Grindelallee 117, 20146 Hamburg, Germany (Received 17 June 2011; published 23 September 2011)

We demonstrate a direct correlation between the charge state and photoluminescence (PL) intensity of individual CdSe nanowires by actively charging them and performing electrostatic force microscopy and PL measurements simultaneously. While the injection of positive charges leads to an immediate PL quenching, a small amount of injected electrons can lead to an increase of the PL intensity. We directly observed the migration of excess charges into the substrate, which leads to a recovery of the PL. Further, we show that the PL of individual NWs can be actively switched between on and off states by charging with the atomic-force microscope tip. We propose a model based on charge trapping and migration into the substrate to explain our results.

DOI: 10.1103/PhysRevLett.107.137403 PACS numbers: 78.67.Uh, 68.37.Ps, 78.55.-m, 78.60.Fi

The photoluminescence (PL) fluctuations of chemically synthesized semiconductor nanostructures such as nanocrystals (NCs) or nanowires (NWs) have been investigated in numerous studies and are attributed to fluctuations of their charge state [1-5]. According to the commonly used model, a photogenerated exciton transfers its recombination energy to an unpaired charge carrier, thus promoting it to an excited quantized state through an Auger mechanism. The charge carrier subsequently thermalizes back to the ground state, rendering the nanostructure dark. In fact, for macroscopic NC films [6,7] and even on the single NC level [8], it has been shown that the injection of electrons leads to a bleaching of the nanocrystal fluorescence. In addition, the charging of individual NCs upon photoexcitation has been directly measured with electrostatic force microscopy (EFM) [9–12]. A direct correlation between the charge state and PL intensity of individual NCs or NWs, however, could not yet be established.

PL experiments on individual nanostructures are mostly performed on CdSe NCs, which have become prototype structures in recent years [13]. Combined EFM and PL measurements are challenging because of both the substrate and the measurement itself. First, the substrate should be flat and conductive for the EFM measurements and, at the same time, it should be optically transparent for the PL investigations. Second, in order to manipulate the charge state, the nanostructure should be charged by an EFM tip. While this is in principle possible [14,15], the simple presence of the metallic tip would influence the optical properties and complicate the PL measurements. These problems are less significant for extended one- or two-dimensional nanostructures with the macroscopic dimensions exceeding the surface roughness. In fact, nanostructures such as carbon nanotubes [16,17] or graphene [18] are well suited for the investigation of the effects of deposited charges because the mobile charges distribute along the nanostructure. The same holds for one-dimensional NWs, as we recently proved by investigating the different mobilities of photogenerated electrons and holes in individual CdSe NWs under local illumination [19]. We observed that the electrons spread over the whole NW while the holes mainly remain at the excitation spot. Mobile charges polarized by an external electric field were also thought to be the reason for local PL intensity changes along individual NWs [20]. However, a direct correlation between the charge state and the PL intensity has not yet been established.

In this letter, we investigate luminescent NWs actively charged by a biased atomic-force microscope (AFM) tip. The charge state is monitored by EFM. We observe that the injection of positive charges as well as large amounts of negative charges leads to PL quenching, whereas a small amount of negative charges can increase the PL. We demonstrate that the PL emission can even be actively switched between on and off by bias modulation.

Figure 1 sketches the sample structure as well as the experimental setup for AFM, EFM, active charging, and optical measurements. Details of the sample preparation can be found in Ref. [19]. Briefly, CdSe NWs grown by

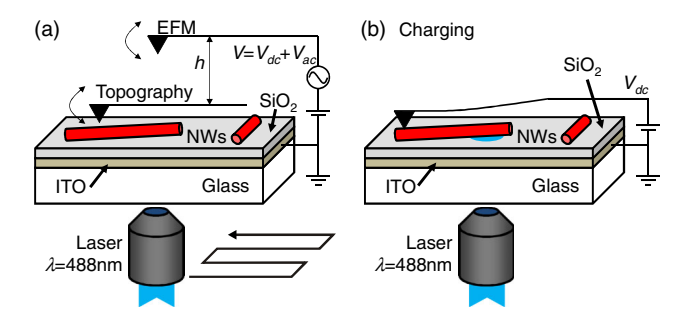


FIG. 1 (color online). Sketch of the sample and the experimental setup. (a) AFM topography and EFM experiments. (b) Charging. The optical measurements were performed either at (a) a confocally scanned or (b) a fixed position of the sample.

the solution-liquid-solid method [21-23] with typical diameters ranging from 7 to 15 nm were used. The NWs were deposited on a substrate consisting of a glass cover slide coated with a thin and flat (rms = 1.3 nm) conductive and optically transparent layer of indium tin oxide (ITO) and an insulating layer of 20 nm SiO₂ prepared by atomic layer deposition [24]. The experimental setup combines an AFM/EFM with a confocal laser scanning microscope (see Ref. [19] for details). In EFM mode [Fig. 1(a)], first the topography line is recorded in a typical AFM scan. On the retrace, the tip is lifted a certain height h, biased, and scanned over the same line at a fixed distance to the sample. The ITO layer is always grounded during EFM and serves as a reference. EFM images are then obtained due to electrostatic forces stemming from the interactions between the sample and the charge on the tip. The contact potential difference between tip and substrate is eliminated by applying a dc voltage to the tip. Applying an additional ac voltage at frequency ω yields two EFM signals that can be separated by means of a lock-in technique. The polarizability signal oscillates at 2ω and the signal at ω solely represents the charge [9,10]. Typically, EFM was performed with an ac voltage of 5 V, ω was set to 800 Hz, the line rate was 0.5 Hz, and the lift height h was 20 nm. Charge injection, sketched in Fig. 1(b), was performed by applying a dc voltage to the tip and pressing it with a few tens of nN on the NW. The transferred charge is then imaged by means of EFM. For some experiments, the PL was recorded while charging by focusing the laser spot on the opposite end of the NW and collecting the PL with the same objective. All experiments were performed at 295 K and under a dry N₂ atmosphere to reduce the migration of the deposited charges along the substrate.

Figure 2(a) depicts an AFM image of a single NW that exemplifies many investigated NWs. Figure 2(b) shows a scanning PL image of the same NW, where only weak PL intensity is visible in the first scan. However, upon further illumination, we observe a photobrightening effect, i.e., an increase in the PL intensity until it saturates. This effect has also been reported for NCs [25,26], but its origin is ambiguous and not the subject of this paper. From the EFM image in Fig. 2(c), it is seen that the NW is still neutral after photobrightening, indicating that there is no connection between photobrightening and charge state. For charging experiments we generally used only NWs with a previously saturated PL intensity [cf. Figure 2(d)]. For all our NWs we observe a spatial PL heterogeneity that has been discussed before [4].

After PL saturation, the NW of Fig. 2 was touched with a negatively biased AFM tip for time periods of 40 s, starting with -2 V and decreasing the voltage in steps of 2 V to -10 V. After each charging step, PL and EFM images were recorded. Figure 2(e) shows the charge image after applying -8 V to the NW. A negative charge distribution spreads uniformly along the direction of the NW axis. The

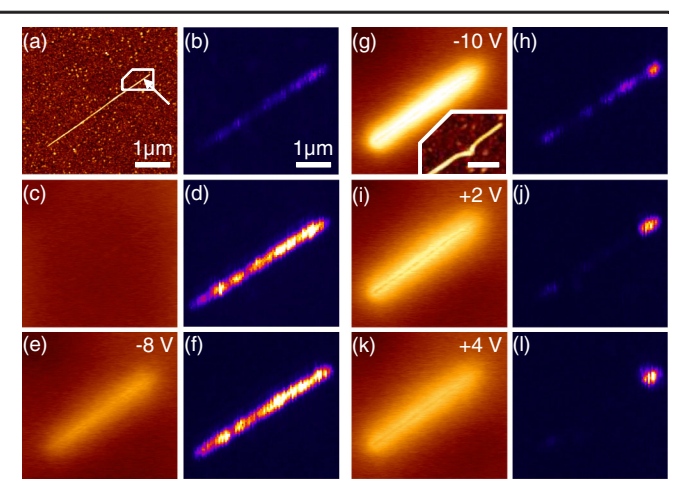


FIG. 2 (color online). (a) AFM, (c),(e),(g),(i),(k) EFM charge, and (b),(d),(f),(h),(j),(l) PL images of a single NW. All EFM and PL images are shown on the same scale. The arrow in (a) indicates the position where the biased tip touched the NW. The inset in (g) displays an AFM image of the area indicated by the white box in (a). The NW is separated, leaving two parts of which only one is further charged. Here, the scale bar is 300 nm. All images have been obtained in an experiment with a specific sequence of charging steps as described in the text.

width of the charge signal, however, is much broader than the NW diameter. For the PL of this NW, we observed no significant change up to -8 V [Fig. 2(f)]. Only if the bias is further decreased to -10 V is the PL visibly decreased [Figs. 2(g) and 2(h)], except for a small bright part on the upper right end of the NW. From the enlarged AFM image in the inset of Fig. 2(g), it can be seen that this small part was separated from the NW by AFM manipulation prior to charging with -10 V. Hence, we conclude that the quenching of the main part of the NW is due to the injection of electrons from the tip. The broadened EFM signal further indicates that a considerable amount of charges spread into the substrate.

Subsequently, positive voltages of +2 V and +4 V were applied to the same NW. From the corresponding EFM and PL images in Figs. 2(i)–2(l), it can be seen that the PL is strongly quenched, except for the separated upper right part of the NW. However, the sample is still negatively charged, although less strongly than before. This is due to substrate charging, which will be discussed later. We note that NWs that have not been charged before show the same behavior, meaning that an irreversible drastic PL decrease occurs after applying the same positive voltages.

In order to gain insight into the dynamics of positive charging and PL quenching, the PL was recorded at one end of a NW while biasing it at the other end. Control experiments with a grounded tip showed no effect on the PL of the NW. Figure 3(a) shows the evolution of the PL intensity of a single NW that has subsequently been tip-biased with +2 V, +3 V, and +4 V for 5 s (highlighted in red). The PL decreases for all voltages immediately after

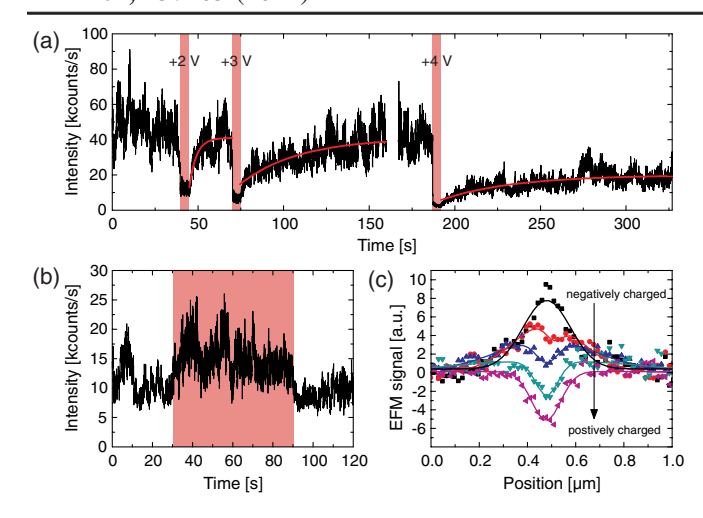


FIG. 3 (color online). (a) PL time trace recorded at one end of a single NW while the other end was biased with +2 V, +3 V, and +4 V for 5 seconds, each (highlighted in red). (b) PL time trace of another NW biased with -4 V from 30 to 90 s. (c) Cross sectional EFM signals of a charged NW. The NW was charged with -0.6 V for 60 s (top curve) and then successively with a positive voltage. Each curve has been fitted with two Gaussian functions to account for negative and positive charges.

the biased tip touches the NW. After applying +2 V and +3 V, the PL recovers almost to its initial level, whereas it approaches a considerably lower level after applying +4 V. A further increase of the voltage leads to lower PL levels and eventually permanent PL quenching. The higher the voltages or the longer a given voltage is applied (not shown here) the longer it takes for the PL to reach a constant level. The PL recovery follows an exponential law with a time constant in the range of seconds, strongly depending on the exact charging parameters. Further experiments reveal that when the NW is imaged while the biased tip still injects charges, the injection position is the first to be quenched permanently and irreversibly. This hints that an irreversible chemical reaction, probably oxidation [27], of highly positively charged NWs leads to nonfluorescent NWs.

Figure 3(b) shows the change of the PL intensity of a NW upon applying a negative bias. Here the tip was biased with -4 V and touched the NW for 60 s. Even though the PL intensity is strongly fluctuating (blinking) as mentioned in the introduction already, it can clearly be seen that the PL is slightly enhanced during the period when the tip actually touches the NW (highlighted in red) and that it recovers to its initial value after the tip is retracted. In contrast to the recovery after biasing with positive voltages, the PL recovers almost immediately. We note that the enhancement effect cannot be seen in the PL images in Fig. 2 since these were not taken with the tip in contact.

Considering the experimental observations shown, we suggest the following model. We assume that the NWs exhibit trap states for electrons. In PL experiments on uncharged NWs, these traps are filled by photogenerated

electrons. This leads to an excess of mobile positive charges within the NWs that in turn opens Auger-like nonradiative recombination channels for photogenerated electron-hole pairs, effectively decreasing the PL intensity. By touching the NWs with a biased tip, charge carriers are injected and distribute along the NW. Small amounts of electrons enhance the PL of NWs by filling the electron traps. Once all traps are filled, additional mobile electrons are injected into the NWs. These additional electrons then quench the PL via the Auger mechanism. The considerably reduced fluorescence by even small amounts of injected holes is explained by a lack of hole trap states, while the fluorescence recovery and substrate charging observed on a longer time scale is due to migration of charges from the NW into the substrate.

We now discuss the migration of the charges into the substrate as observed in Figs. 2(i) and 2(k), where the NWs are more positively charged than the negatively charged surrounding. The charge profiles in Fig. 3(c) are extracted from several EFM line scans perpendicular to a NW axis. As the initially negatively charged NW is subsequently charged with positive voltages, the overall EFM signal decreases [top to bottom in Fig. 3(c)], leaving a halo around the NW (blue curve). Further injection then charges the NW as well as the substrate positively. The halo originates from the remaining negative charges in the substrate making it difficult to clearly differentiate between the charges on the NW and those in the substrate, a problem that has been addressed before already [17,28].

From these observations, we deduce that only a small amount of the injected charges remain in or on the NW while the majority of charge carriers migrate into the substrate. Since the EFM images in Fig. 2 show a uniform distribution of the charges along the NW, the motion of charges along the NW axis is much faster than the migration into the substrate. This is in agreement with previous experiments where it was shown that photogenerated charge carriers distribute rapidly along the NW axis [19]. The transfer of holes (electrons) to the substrate is a slow (fast) process as can be deduced from the PL recovery after tip retraction [see Figs. 3(a) and 3(b), respectively]. Qualitatively, the PL recovery after applying a positive voltage can be explained by regarding the NW and the substrate as a capacitor and a parallel connected resistor that accounts for a leakage current. This current should lead to an exponential decay of positive charge carriers and, consequently, to an exponential PL recovery, if one assumes that the PL intensity is inversely proportional to the amount of excess charges. The more charge carriers are stored in the substrate, the slower the neutralization of the NW will be. This eventually leads to larger time constants for the PL recovery, as is experimentally observed.

Obviously, the PL can be switched on or off by injecting charge carriers in different voltage regimes. To investigate the time scale for possible PL intensity modulations, we

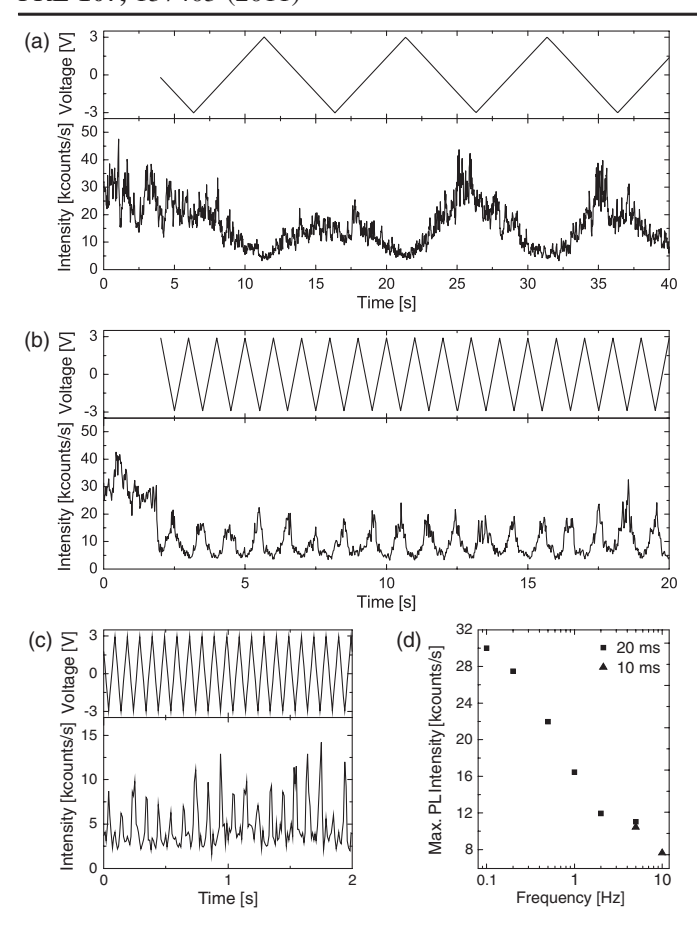


FIG. 4. PL time traces recorded with the biased tip in contact with the NW. Frequencies were (a) 0.1, (b) 1, and (c) 10 Hz. The tip is not in contact with the NW at the beginning of (a) and (b). Time bin is 20 ms for (a) and (b) and 10 ms for (c). The background of approximately 1.3 kcounts/s is attributed to the AFM laser diode that could not be turned off while charging the NW. (d) Maximum average PL for different frequencies. The time bin was changed from 20 to 10 ms at 5 Hz. The maximum intensities for both time bins at 5 Hz are in good agreement, demonstrating that the time bin did not affect the maximum intensity at the chosen frequencies.

applied triangular ac voltages (extremal values ± 3 V) of different frequencies to the tip contacting one side of the wire and recorded the PL on the opposite side. Figure 4(a)–4(c) exemplarily depicts time traces obtained for 0.1 Hz, 1 Hz, and 10 Hz, respectively, revealing PL intensity modulations in all cases. Interestingly, Fig. 4(a) indicates a maximum in the PL intensity slightly before -3 V is reached. This is consistent with the results observed for constant negative voltages where the PL is enhanced for small negative voltages and decreased for large negative voltages.

For higher frequencies, we observe that the voltage minimum and the PL maximum directly correlate and the maximum PL intensity decreases with increasing frequency as summarized in Fig. 4(d). This behavior is consistent with the observed charge carrier migration as

discussed above. Injected holes migrate to the substrate very slow while electrons migrate almost immediately [see Figs. 3(a) and 3(b)]. For low frequencies, the amount of stored charges is closely related to the applied voltage since both electron and hole have enough time to migrate to the substrate. For higher frequencies, however, the slow migration of the holes leads to a constant level of holes stored into the NW. Injection of small amounts of electrons then only leads to a slight enhancement as compared to the positively charged NW. Once the tip has been retracted, the remaining holes migrate to the substrate and in turn restore the initial NW PL.

In summary, we have shown that the PL intensity of single CdSe NWs can be actively quenched by the injection of charge carriers from a biased AFM tip. While the injection of positive charges leads to an immediate PL quenching, a small amount of injected electrons can even lead to an increase of the PL, which is explained by a trap filling model. Further, we directly observed the migration of excess charges into the substrate, which can lead to a recovery of the PL to its initial value. This combination of local optical and electrical measurements, together with electrical manipulation, provides a new tool to understand the opto-electrical properties of nanostructures.

The authors thank Kornelius Nielsch and Robert Zierold (financed through the Excellence Cluster "Nanotechnology for Medicine") from the Institute of Applied Physics of the University of Hamburg for depositing the SiO₂ layers on the substrates. This work was supported by the DFG via ME 1380/16-1.

- [1] M. Nirmal et al., Nature (London) 383, 802 (1996).
- [2] A.L. Efros and M. Rosen, Phys. Rev. Lett. 78, 1110 (1997).
- [3] P. Frantsuzov et al., Nature Phys. 4, 519 (2008).
- [4] V. V. Protasenko et al., Adv. Mater. 17, 2942 (2005).
- [5] J. J. Glennon et al., Nano Lett. 7, 3290 (2007).
- [6] C. J. Wang et al., Science 291, 2390 (2001).
- [7] P. P. Jha and P. Guyot-Sionnest, J. Phys. Chem. C 111, 15 440 (2007).
- [8] P. P. Jha and P. Guyot-Sionnest, J. Phys. Chem. C 114, 21 138 (2010).
- [9] T.D. Krauss and L.E. Brus, Phys. Rev. Lett. 83, 4840 (1999).
- [10] T. D. Krauss et al., J. Phys. Chem. B 105, 1725 (2001).
- [11] O. Cherniavskaya et al., Nano Lett. 3, 497 (2003).
- [12] S. Li et al., ACS Nano 3, 1267 (2009).
- [13] D.E. Gomez *et al.*, Phys. Chem. Chem. Phys. **8**, 4989 (2006).
- [14] E. A. Boer et al., Appl. Phys. Lett. 78, 3133 (2001).
- [15] M. A. Salem et al., Appl. Phys. Lett. 85, 3262 (2004).
- [16] M. Zdrojek et al., Appl. Phys. Lett. 86, 213114 (2005).
- [17] M. Zdrojek et al., J. Appl. Phys. 100, 114326 (2006).
- [18] A. Verdaguer et al., Appl. Phys. Lett. 94, 233105 (2009).
- [19] S. Schäfer et al., Nano Lett. 11, 2672 (2011).

- [20] V. Protasenko et al., J. Am. Chem. Soc. 129, 13160 (2007).
- [21] T.J. Trentler et al., Science 270, 1791 (1995).
- [22] F.D. Wang et al., Inorg. Chem. 45, 7511 (2006).
- [23] Z. Li et al., Adv. Funct. Mater. 19, 3650 (2009).
- [24] J. Bachmann *et al.*, Angew. Chem., Int. Ed. **47**, 6177 (2008).
- [25] J. Jasieniak and P. Mulvaney, J. Am. Chem. Soc. 129, 2841 (2007).
- [26] V. Biju et al., J. Phys. Chem. C 111, 7924 (2007).
- [27] L. Spanhel et al., J. Am. Chem. Soc. **109**, 5649 (1987).
- [28] M. Zdrojek *et al.*, Phys. Rev. Lett. **96**, 039703 (2006).